Article

Not peer-reviewed version

Impaired Coordination of the Ciliary Movement in Patients with Chronic Rhinosinusitis with Nasal Polyps: The Role of Decreased Planar Cell Polarity Protein Expression

Sakura Hirokane , Tomohiro Kawasumi , Sachio Takeno * , Yukako Okamoto , Seita Miyamoto , Rikuto Fujita , Chie Ishikawa , Takashi Oda , Yuichiro Horibe , Takashi Ishino , Takao Hamamoto , Tsutomu Ueda

Posted Date: 24 July 2024

doi: 10.20944/preprints202407.1890.v1

Keywords: paranasal sinus; chronic rhinosinusitis; nasal polyps; ciliated cell; mucociliary clearance; planar cell polarity; CPLANE complex proteins; WDPCP; FUZ; type 2 inflammation

Article

Impaired Coordination of the Ciliary Movement in Patients with Chronic Rhinosinusitis with Nasal Polyps: The Role of Decreased Planar Cell Polarity Protein Expression

Sakura Hirokane [1], Tomohiro Kawasumi [1], Sachio Takeno [1,*], Yukako Okamoto [1], Seita Miyamoto [1], Rikuto Fujita [1], Chie Ishikawa [1], Takashi Oda [1], Yuichiro Horibe [1], Takashi Ishino [1], Takao Hamamoto [1] and Tsutomu Ueda [1]

[1] Department of Otorhinolaryngology, Head and Neck Surgery, Graduate School of Biomedical Sciences, Hiroshima University, Hiroshima 734-8551, Japan

* Correspondence: takeno@hiroshima-u.ac.jp; Tel.: +81-82-257-5252; Fax: +81-82-257-5254

Abstract: The planar cell polarity (PCP) of epithelial ciliated cells is essential for effective mucociliary clearance (MCC) in the sinonasal mucosa. We hypothesize that MCC coordination is impaired in nasal polyp (NP) mucosae due to suppressed expression of a series of CPLANE (ciliogenesis and planar cell polarity effector) complex proteins in chronic rhinosinusitis (CRS) patients. To investigate this hypothesis, we subjected sinonasal mucosal samples to live video recording to measure mucociliary transport velocity (MCTV) and scanning electron microscopy to evaluate surface morphology. The expression and distribution of a panel of PCP proteins, e.g., WDPCP and FUZ, were investigated in relation to inflammatory cytokine levels and clinical features. The mean MCTV of NP mucosae was significantly lower than that of the inferior turbinate mucosae. The CRS group with NPs (CRSwNP group) (n=28) showed increased expression of IL-13 and CCL26 mRNA compared to CRS patients without NPs (n=25) and controls (n=30). WDPCP and FUZ mRNA levels were significantly decreased in NP mucosae compared to ethmoid sinus mucosae in CRSwNP patients. WDPCP protein distribution was reduced in the cytoplasmic region of ciliated cells in CRSwNP patients. We conclude that suppression of WDPCP in ciliated cells is responsible for the impaired MCC of nasal polyps with type-2 inflammation. This mechanism might explain the decreased clearance and the potential for worsening symptoms of CRSwNP.

Keywords: paranasal sinus; chronic rhinosinusitis; CRS; nasal polyps; ciliated cell; mucociliary clearance; planar cell polarity; CPLANE complex proteins; WDPCP; FUZ

1. Introduction

The sinonasal cavity is the front line of defense of the human respiratory tract. Host–pathogen interactions occur with every breath of ambient air, which contains aerosolized fungal spores, bacteria, virus particles and other noxious pathogens [1,2]. The sinonasal mucosa is physically protected by a physiological barrier system known as mucociliary clearance (MCC). This system consists of three fundamental functional components: the production of mucin, ceaseless ciliary activity, and the airway surface liquid layer [3].

Chronic rhinosinusitis (CRS) is one of the most common chronic inflammatory diseases, affecting approximately 10% of the population worldwide [4,5]. In Japan, roughly 0.05% of the population and approximately 3–4% of children suffer from sinusitis [4]. CRS affects quality of life (QOL) [6], not only due to local symptoms such as nasal discharge, nasal congestion, headaches and hyposmia, but also due to systemic impairment such as general fatigue.

The complexity of CRS pathology has been elucidated by ongoing research efforts to unveil the etiology and pathophysiology of the disease [7–9]. The emerging view is that CRS is a heterogenous syndrome resulting from a dysfunctional interaction between various environmental factors and the

 doi:10.20944/preprints202407.1890.v1

host immune system [10,11]. In this sense, the presence of nasal polyposis constitutes a differentiating phenotype. Indeed, CRS has historically been divided into 2 main phenotypes on the basis of the presence or absence of nasal polyps (NPs): CRS with NPs (CRSwNP) and CRS without NPs (CRSsNP) [12–16]. Nasal polyps typically manifest after prolonged periods of local CRS inflammatory processes. Patients with CRSwNP suffer prolonged severe nasal symptoms and generally show a poor response to medical and surgical intervention compared to those with CRSsNP [13,17–19].

The functional importance of the sinonasal epithelial mucosa in the pathogenesis of CRS is now clearly established. The past several decades have witnessed a gradual but definitive shift in our view of its role from that of a passive barrier to that of an active immunologic organ with both innate and adaptive components [20,21]. Multiple studies have demonstrated evidence for barrier dysfunction in the setting of CRS characterized by both a reduction in epithelial cellular junctions and increased susceptibility [22–25]. These degenerative changes induce significant loss of the differentiation of basal cells into ciliated cells, compromise the barrier function of the surface mucosa, and reduce MCC efficacy [26,27].

Ciliated epithelial cells of the respiratory tract exhibit asymmetrical polarity of two types: polarity along the apical–basal axis and polarity along the horizontal plane of the epithelial sheet [3]. The latter is referred to as planar cell polarity (PCP). This PCP is an essential property that regulates the directionality of MCC as well as epithelial tissue integrity [28]. The physiological process of ciliary beating is coordinated temporally and spatially to exert effective mucociliary transport function. The property of PCP is closely related to the functional expression of a series of CPLANE (ciliogenesis and planar cell polarity effector) complex proteins. These include the Inturned (inturned planar cell polarity protein), Fuz (fuzzy planar cell polarity) and WDPCP (WD repeat containing planar cell polarity effector) proteins [29–32].

While aberrant structural morphology of the cilia together with ciliary beating dysfunction has been characterized as part of CRS pathology [33], it remains unclear how the expression and distribution of CPLANE proteins are altered in the ciliated cells of NP mucosa. In particular, it has yet to be elucidated how PCP directionality is affected by the NP formation process under type 2 inflammation.

The aim of this study is, therefore, to improve our understanding of the molecular pathways involved in MCC integrity and the role of the CPLANE proteins by identifying their complex interactions with various inflammatory mediators in CRS. We report that mucociliary transport is suppressed in nasal polyps in conjunction with decreased expression and distribution of WDPCP transcripts. Our findings might pave the way for potential therapeutic interventions aimed at PCP restoration. Through our comprehensive analyses, we hope to provide valuable insights into this field and ultimately advance the development of targeted therapies for patients suffering from this debilitating condition.

2. Patients and Methods

2.1. Study Design and Tissue Samples

This was a case-control study of 53 CRS patients and 30 control subjects who underwent endoscopic endonasal sinus surgery. We obtained tissue samples from the ethmoid sinus, nasal polyps (if any), and the inferior turbinate at the time of surgery. When CRS findings were identified bilaterally, specimens were taken from both sides. The CRS diagnosis was based on the patient's history, clinical referral symptoms, endoscopic nasal findings, and computed tomography (CT) images [34]. Patients with previous sinus surgeries were excluded. None of the patients had received systemic or topical steroids for ≥4 weeks prior to the surgery. The severity of CRS was assessed from CT images by radiological grading using the 24-point Lund-Mackay system [35]. The presence of allergic rhinitis (AR) was diagnosed based on the patient's clinical history, the presence of nasal symptoms together with positive nasal eosinophils, and positive allergen-specific IgE antibodies against common airborne allergens. We classified the CRS patients into CRSsNP and CRSwNP phenotypes [11]. Thirty patients without sinus infectious diseases who underwent endonasal surgery

 doi:10.20944/preprints202407.1890.v1

served as controls. They all had normal-appearing paranasal sinus mucosae with normal radiological findings. The control subjects' histories included surgery for nasal obstruction (n=18), orbital decompression for dysthyroid ophthalmopathy (n=4), endoscopic dacryocystorhinostomy (DCR) (n=4), endonasal surgery for an intraorbital or sphenoid benign tumor (n=3) and fibrodysplasia ossificans progressiva (n=1).

2.2. Mucociliary Transport Velocity (MCTV) Measurement

Sinonasal mucosal strips were prepared for live video recording to measure mucociliary transport velocity (MCTV) and direction. For this purpose, mucosal strips of the lateral-side inferior turbinate and nasal polyps were trimmed under a stereoscopic microscope into approximately 3- x 5-mm rectangles, with the surface mucosa remaining intact. The sectioning technique ensured that the antero-posterior and supero-inferior directions remained fixed for each specimen. Great care was taken to avoid any surface trauma. The mucosal strips were immersed in PBS and transferred into 35-mm dish chambers filled with medium specifically for culturing human nasal epithelial cells (C-21160; PromoCell, Heidelberg, Germany). We used charcoal powder with grains of approx. 10 μm diameter as a tracer. The transport direction and velocity created by ciliary beating were observed under a Zeiss Observer D1 Inverted optical microscope (Zeiss, München, Germany) equipped with a DP72 EVIDENT® digital imaging system (Olympus, Tokyo). We recorded 4–5 sessions of 5 min duration for each specimen. The recording data were analyzed by cellSens® ver. 1.5 image software (Olympus). The MCTV of each mucosal strip was determined by measuring the traveled distance of charcoal microparticles per unit time. All procedures were performed at room temperature (approx. 27°C) and completed within 6 h after sample collection.

2.3. Scanning Electron Microscopy (SEM)

Tissue specimens were carefully removed from patients and placed in fixative (2.5% glutaraldehyde, 2% paraformaldehyde in 0.1 M phosphate buffer, pH 7.4) for SEM observation. After initial fixation, the specimens were rinsed in distilled water 3 times followed by post-fixation with 2% osmium tetroxide for 2 h. After dehydration through a graded ethanol series (50%, 70%, 80%, 90%, 95% and 100%), specimens were immersed in t-butanol for 1.5 h, then dried in a t-butanol freeze-drying device (VFD-21S; Vacuum Device Inc., Ibaraki, Japan). Specimens were sputter-coated with osmium (Neoc-ST; Meiwa Forsys, Tokyo) and observed under a JBL-7800F scanning electron microscope (JEOL Ltd., Tokyo).

Cell types were recorded, and their relative proportions were determined as mean percent surface area. Ciliary synchronization, defined as percent of cilia "in phase" with the metachronal pattern of the specimen, was also evaluated after whole-surface scanning as described elsewhere [36].

2.4. Total RNA Extraction and Quantitative RT-PCR Analysis

The surgical specimens were divided and immersed in RNAlater™ solution (Thermo Fisher Scientific, Waltham, MA) for reverse transcription-polymerase chain reaction (RT-PCR). A quantitative PCR analysis was performed on an ABI Prism 7300 system (Applied Biosystems, Foster City, CA) as previously described [34]. Cellular RNA was isolated using RNeasy mini-kits (Qiagen, Valencia, CA). Total RNA was then reverse-transcribed to cDNA using a high-capacity RNA-to-cDNA kit (Applied Biosystems) according to the manufacturer's instructions. Gene expressions were measured on a real-time PCR system using TaqMan Gene Expression Assays (Thermo Fisher Scientific). PCR primers specific to WDPCP (Hs00210831_m1), FUZ (Hs00228395_m1), IL-13 (Hs00174379_m1), CCL26 (Hs00171146_m1), and IL-1β (Hs01555410_m1) were used (Thermo Fisher Scientific). GAPDH (Hs02786624_g1) was used as a reference gene. Amplifications of the PCR products were quantified by the number of cycles, and the results were analyzed using the comparative cycle threshold (Ct) method ($2^{-\Delta\Delta Ct}$). The target gene expression values are presented as relative ratios compared to the expression of the reference gene (ratio: target gene/GAPDH gene expression).

 doi:10.20944/preprints202407.1890.v1

2.5. Immunohistochemistry and Laser Scanning Confocal Microscopy (LSCM) Imaging

The primary antibodies used were anti-human WDPCP rabbit polyclonal antibody (#CSB-PA528516LA0.1HU; CUSABIO, Houston, TX) and anti-human ac-tubulin mouse monoclonal antibody (#SC-23950; SCB, Dallas, TX).

Mucosal specimens were fixed in 10% neutral buffered formaldehyde for immunohistochemistry. Tissues were embedded in paraffin following ethyl alcohol dehydration and then sectioned to 5 μm thickness. The sections were air-dried overnight at 37°C, followed by deparaffinization, hydration and antigen retrieval. The sections were then immersed in 3% H_2O_2 for 10 min for endogenous peroxidase deactivation and blocked with 10% goat serum in phosphate-buffered saline (PBS) containing 0.1% Tween 20 for 1 h at room temperature (RT). The slides were incubated overnight at 4°C with the primary antibodies. Staining and detection for light microscopy were performed with a universal staining kit and DAB detection system according to the manufacturer's instructions (Histofine Simple Stain kit; Nichirei Biosciences, Tokyo). Sections were counterstained with hematoxylin. Control specimens with IgG1 isotype control were used to verify that nonspecific binding was not detectable. Consecutive sections were routinely stained with hematoxylin-eosin (HE) for the assessment of mucosal pathology and the degree of eosinophil infiltration.

Paraffin-embedded sections were deparaffinized with xylene for laser scanning confocal microscopy (LSCM) imaging as described elsewhere [37]. Briefly, antigen retrieval was performed with antigen retrieval solution at 95°C for 40 min (Histofine antigen retrieval solution pH 9; Nichirei Biosciences, Tokyo). Non-specific binding was blocked by incubating the tissue sections with 10% goat serum for 1 h at room temperature. Tissue sections were then incubated overnight at 4°C with anti-human WGPCP polyclonal antibody (1:100) and anti-human ac-tubulin (1:500). They were then reacted with the appropriate secondary antibodies, including anti-mouse goat IgG Alexa Fluor® 555 (#A32727; Invitrogen, Carlsbad, CA) (1:100) and anti-rabbit IgG goat Alexa Fluor®488 (#A32731; Invitrogen) (1:100). Nuclear staining was done with DAPI (#71-03-00; KPL, Gaithersburg, MD) in PBST with 0.01% sodium azide at room temperature for 1 h. The sections were then washed with PBS and mounted with VECTASHIELD Antifade Mounting Medium (#H-1000-10; Vector Laboratories, CA). Fluorescence-immunolabeled images were acquired using LSCM (Stellaris 5; Leica). Control specimens with IgG1 isotype control were used to verify that nonspecific binding was not detectable.

2.6. Data Analysis

The power and sample size calculations for the study design were performed based on data from reports of inflammatory cytokine expression in CRS patients [202B]. The G*power program ver. 3.1.9.6 was employed for the estimation (https://www.psychologie.hhu.de/arbeitsgruppen/allgemeine-psychologie-und-arbeitspsychologie/gpower.html, accessed May 24, 2024). For multiple comparisons, data were screened for differences using the Kruskal-Wallis test. If the analysis gave a significant result, a further comparison was done either by the Mann–Whitney U-test for between-group analysis or by the Wilcoxon signed-rank test for matched samples. Fisher's exact test was used to compare qualitative data. Correlation coefficients were calculated by the Spearman method. Probability (p)-values <0.05 were considered significant.

All procedures in this study complied with the ethical standards expressed in the Helsinki Declaration. The study protocol was approved by the Institutional Review Board of Hiroshima University School of Medicine (approval no. Hi-136-4; approval date: 2 Nov. 2022). Written informed consent was obtained from all patients prior to their participation.

3. Results

3.1. Background and Characteristics of Subjects in the Study

 doi:10.20944/preprints202407.1890.v1

The background and clinical characteristics of the study population are summarized in Table 1. We classified the 53 CRS patients into CRSsNP (n=25) and CRSwNP (n=28) groups based on phenotype. There were no significant gender, body mass index (BMI), or AR comorbidity differences between the patient groups or between either group and the controls (n=30). Mean age was significantly higher in the CRSsNP group ($p < 0.001$) and the CRSwNP group ($p < 0.01$) than in the control group. The CRSwNP group showed significant differences compared to the CRSsNP and control groups in the rate of asthma comorbidity, CT score ($p < 0.0001$), blood eosinophil count ($p < 0.001$), and tissue eosinophil count ($p < 0.001$).

Table 1. Background and clinical characteristics of the study population.

	controls	CRSsNP	CRSwNP
n (male/female)	30 (17/13)	25 (13/12)	28 (15/13)
Age, mean±SD	44.0 ± 17.7	60.4 ± 15.0†††	54.9 ± 10.2††
BMI, kg/mm^2, mean±SD	22.9±4.0	22.4 ± 2.8	22.6 ± 2.8
Allergic rhinitis, %	19 (63.3%)	12 (48%)	19 (67.8%)
Bronchial asthma, %	2 (6.7%)	0 (0%)	9 (32.14%)**,†
CT score, mean±SD	NA	3.75 ± 3.5	12.75 ± 4.98****
Blood eosinophils, %; median, range	4.4 (0.3–4.4)	1.9 (0.3–14.4)	5.55 (0.3–13.9)***
Tissue eosinophils, cells/HPF; median, range	4.8 (0.0–103.3)	2.6 (0.0–45)	74.2 (0.0–333.3)***

Data are represented as mean ± standard deviation (SD), median (range), or number (%). **p<0.01, ***p<0.001, ****p<0.0001 vs. the other groups. †p<0.05, ††p<0.01, †††p<0.001 vs. the control. BMI, body mass index; HPF, high-power field (x400); CT, computed tomography; NA, not available.

3.2. Mucociliary Transport Velocity Assessment

Mucosal specimens were harvested from 5 inferior turbinates and 5 nasal polyps from 5 selected CRSwNP patients and subjected to MCTV measurements. Figure 1 shows a comparison of MCTV vectors between interior turbinates and nasal polyps. Each vector represents the distance and direction traveled of charcoal microparticles loaded on the mucosal slips. The distribution of the MCTV vectors differed between the two sites. Mucosal strips of the inferior turbinate showed steady transport ability toward the posterior direction with an average inclination angle of 135.0 degrees. On the other hand, vectors of nasal polyp specimens had an average inclination of 190.0 degrees and failed to maintain steady alignments. The mean MCTV of nasal polyps was 98.6 μm/min, which was significantly less than that of the inferior turbinate mucosae (210.8 μm/min, $p < 0.01$) **(*Figure 2*)**.

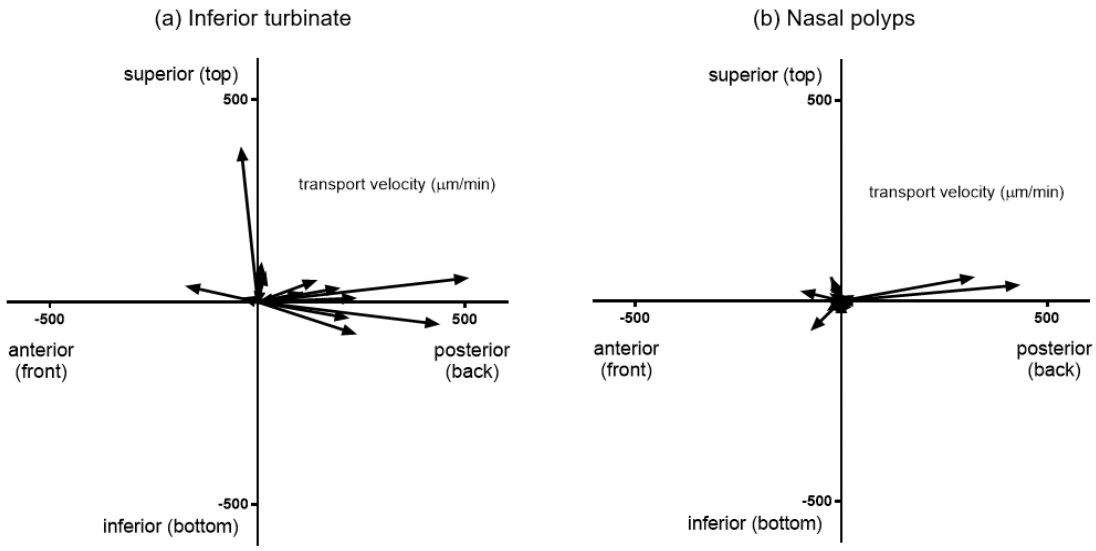

 doi:10.20944/preprints202407.1890.v1

Figure 1. Comparison of mucociliary transport velocity (MCTV) vectors for each mucosal specimen between interior turbinates **(a)** and nasal polyps **(b)**. The MCTV was calculated by 3 recording sessions for each mucosal strip. The distribution of the MCTV vectors differs between the two groups. The majority of the inferior turbinate mucosae showed steady transport ability in the posterior direction. On the other hand, vectors of nasal polyp specimens failed to maintain regular alignments.

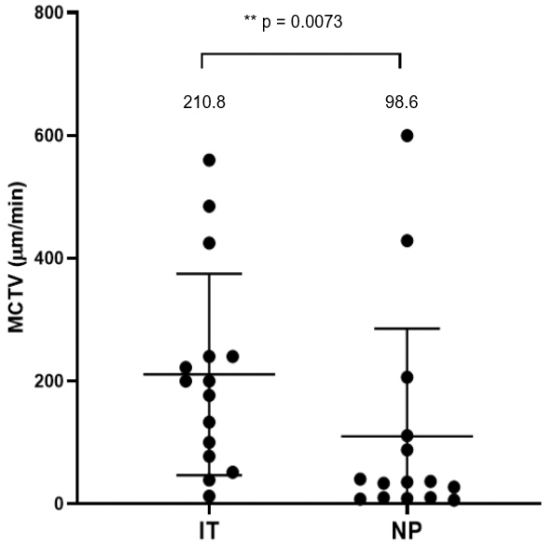

Figure 2. Comparison of mucociliary transport velocity (MCTV) between the inferior turbinate and nasal polyps. *p<0.05. Center lines: mean values. Error bars: standard deviations. IT, inferior turbinate; NP, nasal polyps.

3.3. SEM Observation

Four surface cell types were identified by SEM observation: ciliated cells, unciliated microvillous cells, secretory goblet cells, and squamous cells. Representative SEM photomicrographs showing the surface morphology and cell types of the inferior turbinate and nasal polyp mucosa are presented in Figure 3. The inferior turbinate mucosa tended to have a "ciliated cell-dominant" appearance. The cilia were of uniform length and few developing short cilia were seen. Appearance of ciliary synchronization as revealed by the typical metachronal pattern was generally well-maintained. On the other hand, the nasal polyp mucosa in the CRSwNP group showed wide variation in the relative proportions of cell types among specimens. The surface of individual specimens, however, was consistent in appearance. The degree of synchronization of cilia also varied and was relatively poor with random orientation.

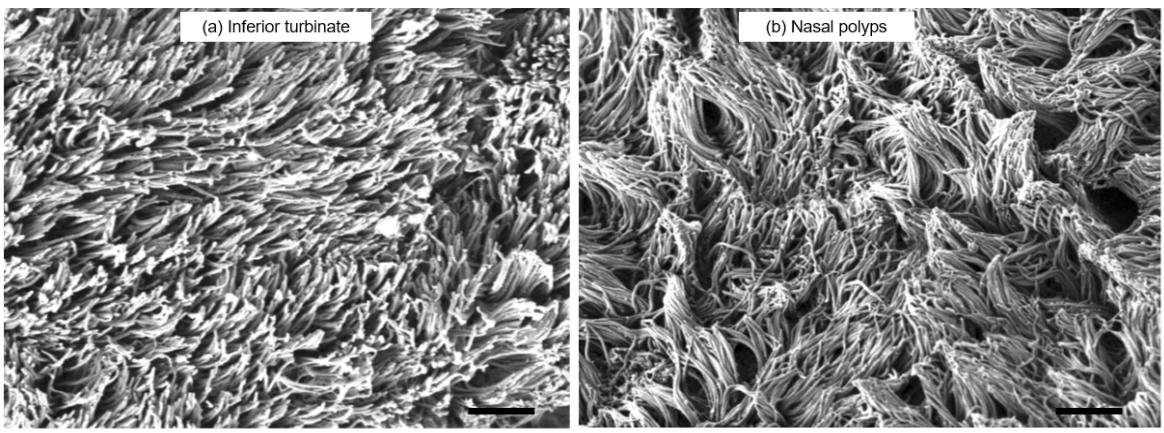

 doi:10.20944/preprints202407.1890.v1

Figure 3. Representative SEM photomicrographs showing surface morphology and cell types. **(a)** Inferior turbinate mucosa from a subject in the control group showing a "ciliated cell-dominant" appearance. Ciliary synchronization as revealed by the typical metachronal pattern is generally well-maintained. **(b)** Nasal polyp mucosa from a patients in the CRSwNP group. The vast majority of the luminal surface is covered by dense cilia; however, the synchronization of the cilia is relatively poor with random orientations. Scale bars: 10 μm.

3.4. Target Gene Expressions in Sinonasal Mucosa and Nasal Polyps

3.4.1. Comparison of mRNA Expressions of PCP Proteins between the Controls and CRS Patients

We classified the ethmoid sinus mucosa and nasal polyp (NP) samples obtained at surgery into a control group, a CRSsNP group and a CRSwNP group. We conducted RT-PCR analysis to determine the mRNA expression levels of WDPCP, FUZ, IL-13, CCL26, and IL-1β. The results showed that WDPCP transcripts were significantly decreased in the NP tissue of the CRSwNP group as compared to the ethmoid sinus mucosa of all the three groups. In CRSwNP patients, a significant decrease in FUZ expression was also observed in the NP tissues as compared to those in the ethmoid mucosae of the same patients (**Figure 4a,b**). The expressions of IL-13 and CCL26 were higher in the NP and ethmoid sinus mucosa of the CRSwNP group compared to those of the control and CRSsNP groups. No significant difference among the three groups was observed in the IL-1β expression level (**Figure 4c,d,e**).

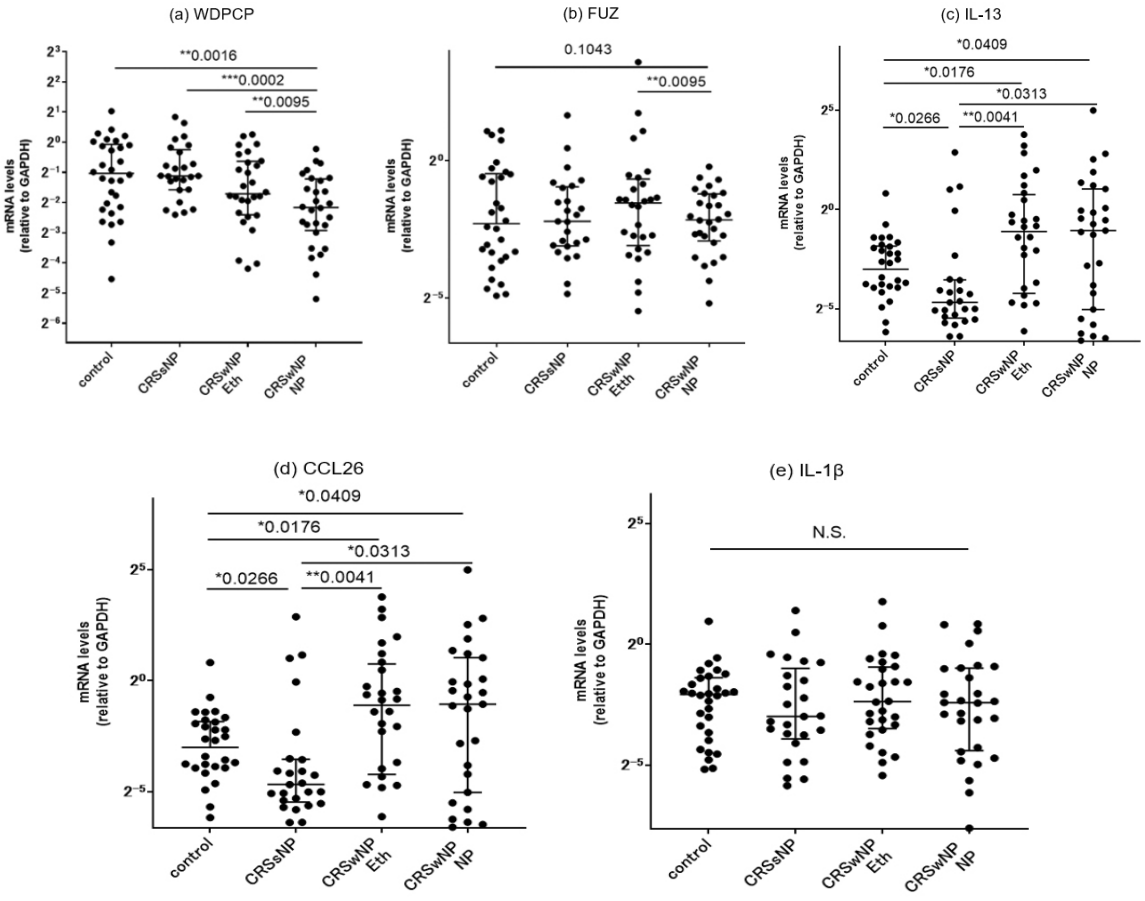

Figure 4. Comparison of the mRNA expressions in paranasal sinus mucosae from the controls, CRSsNP patients, and CRSwNP patients as detected by RT-PCR. The **(a)** WDPCP, **(b)** FUZ, **(c)** IL-13, **(d)** CCL-26 and **(e)** IL-1b mRNA levels were quantitatively normalized against GAPDH levels. *p<0.05, **p<0.01, ***p<0.001. *Center lines:* median values. *Error bars:* interquartile ranges. CRS, chronic rhinosinusitis; Eth, ethmoid; NP, nasal polyps.

 doi:10.20944/preprints202407.1890.v1

We further subdivided the surgical specimens from the CRSwNP patients into the three different areas and compared the mRNA expression levels of the PCP proteins based on the regional differences. Nasal polyp specimens in this group showed a significant downregulation of WDPCP and FUZ levels compared to the ethmoid sinus mucosae obtained from the same patients. A similar comparison was performed against the inferior turbinate mucosae; no significant between-site differences were observed (**Figure 5**).

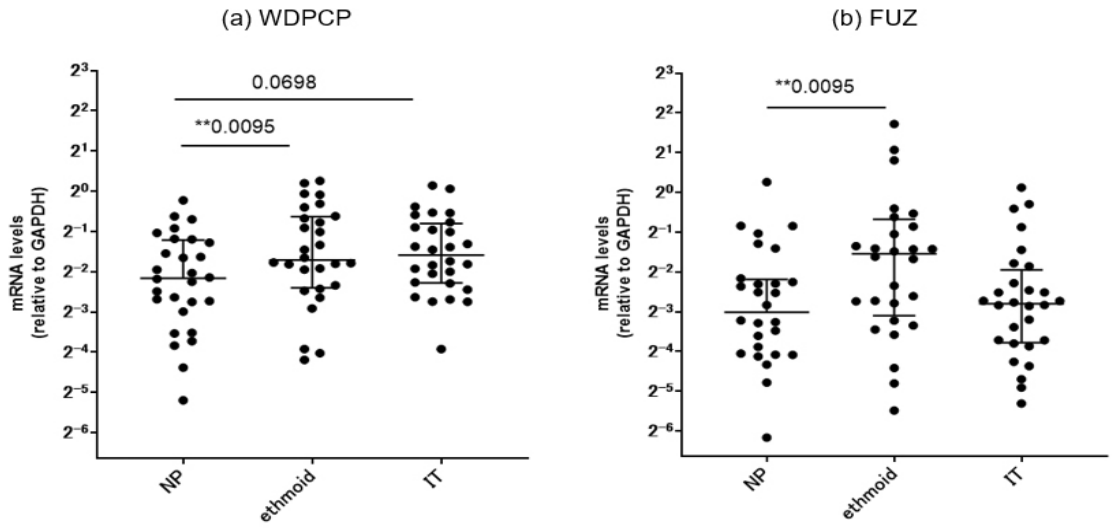

Figure 5. Comparison of the mRNA expression levels in nasal polyps, ethmoid sinus mucosae, and inferior turbinate mucosae for each patient in the CRSwNP group. **(a)** WDPCP and **(b)** FUZ. *p<0.05, **p<0.01. *Center lines:* median values. *Error bars:* interquartile ranges. NP: nasal polyps, IT: inferior turbinates.

3.4.2. Correlation with Inflammatory Cytokines

We further conducted a correlation analysis to assess possible associations among the mRNA-expression levels of IL-13, CCL26, IL-1β and PCP proteins sampled from the same surgical specimens in the CRS patients (**Figure 6**). Notably, we observed a close positive correlation between WDPCP and FUZ (r=0.7267). On the other hand, both WDPCP and FUZ exhibited no significant correlations with IL-13, CCL26 or IL-1β.

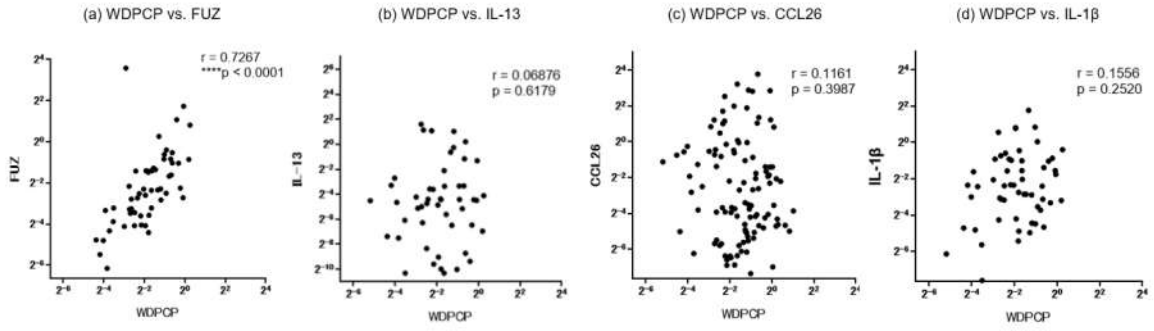

 doi:10.20944/preprints202407.1890.v1

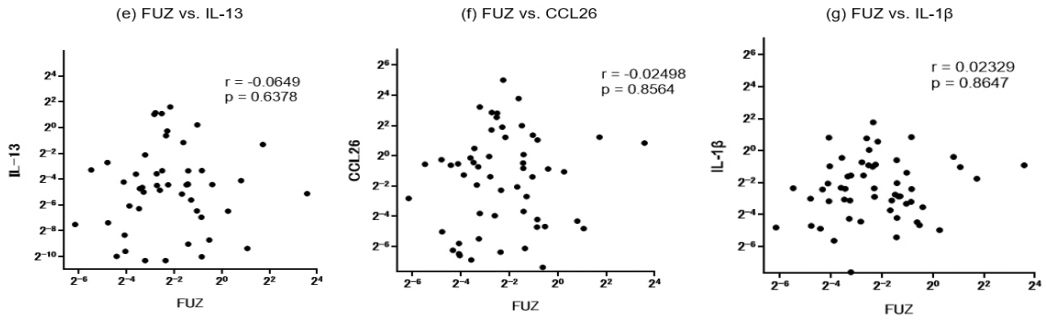

Figure 6. a–d: Correlation of mRNA expression levels between WDPCP and a panel of inflammatory cytokines in ethmoid sinus and nasal polyp mucosae from all CRS patients. **e–g**: Correlations of mRNA expression levels between FUZ and a panel of inflammatory cytokines in ethmoid sinus and nasal polyp mucosae from all CRS patients. CRS: chronic rhinosinusitis.

3.5. Immunohistochemistry and Laser Scanning Confocal Microscopy (LSCM) Imaging

Since decreases in transcription of WDPCP were associated with type 2 inflammation of CRSwNP pathology and clinical manifestations, we examined the paranasal sinus tissue distribution of WDPCP proteins. Patients in the CRSwNP group predominantly showed dense eosinophil infiltration on conventional histological examination. By contrast, intense inflammatory cell infiltration with neutrophils and lymphocytes dominated the ethmoid mucosae in CRSsNP patients. Representative immunohistological images of the WDPCP distribution in ethmoid sinus mucosae and nasal polyp tissues are provided in Figure 7. Ciliated cells of the epithelial layers were stained positively for WDPCP. In contrast, secretory goblet cells in the epithelial layer generally showed lack of staining. Higher rates of intense staining were observed in the ciliated cells of control subjects along the luminal surface.

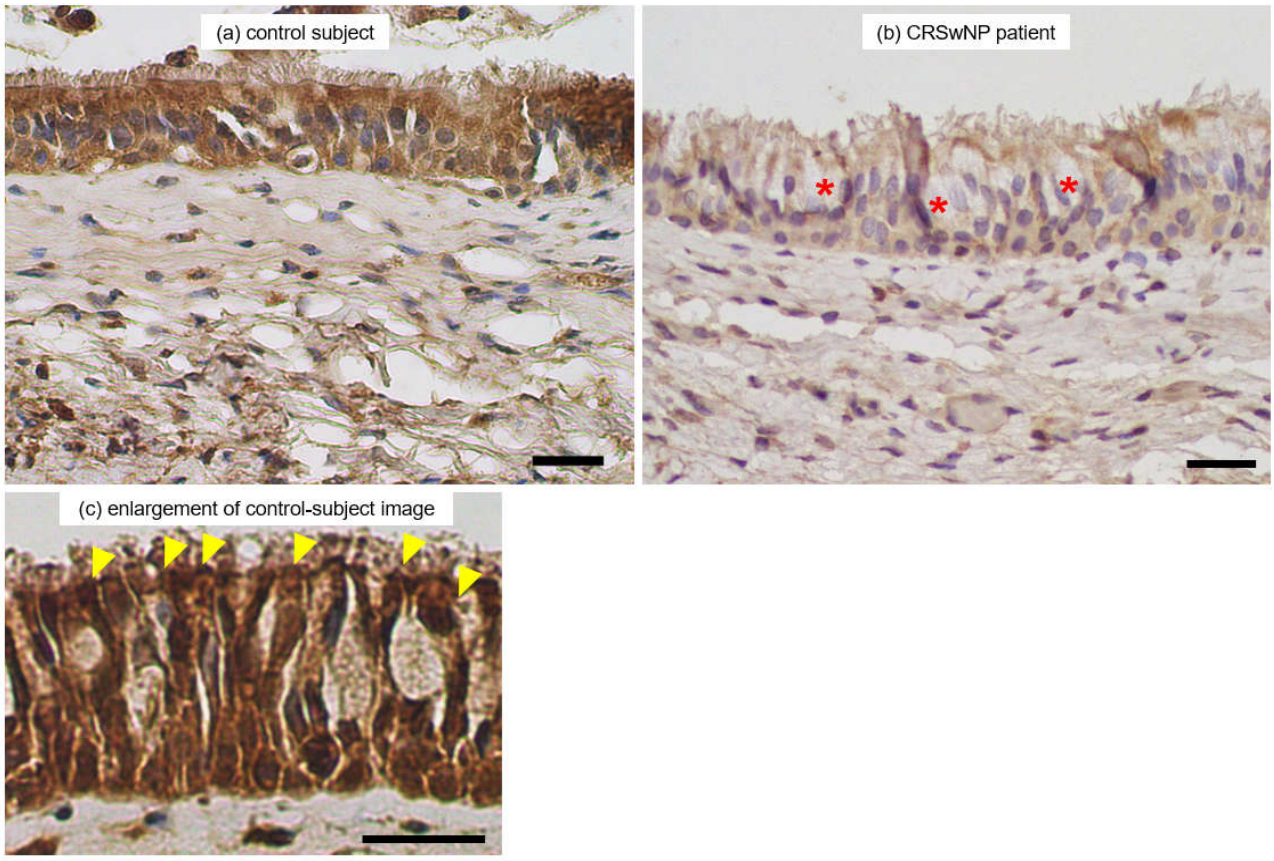

Figure 7. Representative immunohistological images showing WDPCP expression in an ethmoid sinus mucosa sample from a control subject **(a)** and a nasal polyp from a CRSwNP patient **(b)**. Ciliated

 doi:10.20944/preprints202407.1890.v1

cells of the epithelial layers are stained positively for WDPCP. Higher rates of intense staining are observed in the ciliated cells of control subjects along the luminal surface in enlarged views **(Figure 7c, arrowheads)**. In contrast, secretory goblet cells in the epithelial layer generally show lack of staining **(Figure 7b, asterisks)**. Scale bars: 20 μm.

We further examined the distribution and colocalization of WDPCP and ac-tubulin, a marker for epithelial cilia, by LSCM because WDPCP production was closely related to ciliated cell morphology. LSCM images showed that WDPCP protein was observed in the cytoplasmic region of ciliated cells and partially colocalized with ac-tubulin protein **(Figure 8)**. WDPCP distribution was reduced in the epithelial layer of the CRSwNP patients compared with that in control subjects.

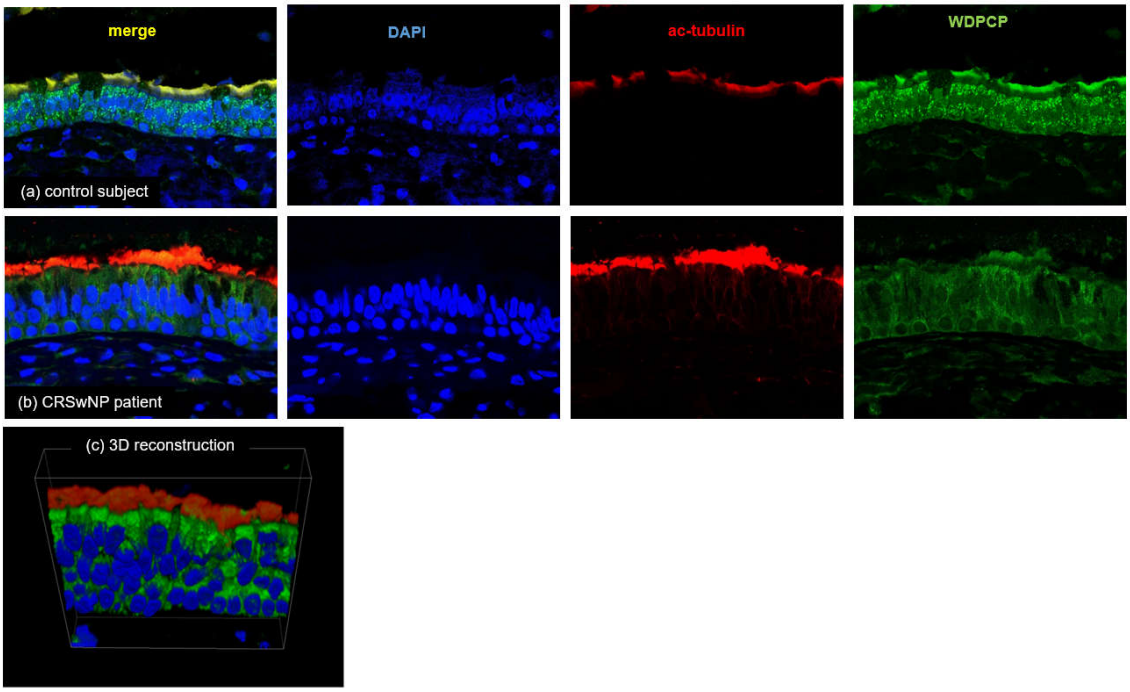

Figure 8. Representative LSCM images showing production and localization of WDPCP (green fluorescence) and ac-tubulin (red fluorescence) in an ethmoid sinus mucosa sample from a control subject **(a)** and in nasal polyps from a CRSwNP patient **(b)**. WDPCP distribution is mainly observed in the cytoplasmic region of epithelial ciliated cells and partially colocalized with ac-tubulin protein (yellow) in the ciliated cells. Higher degrees of staining are observed in the control subjects. **(c)** An enlarged 3D image of the control subject. Nuclei are counterstained with DAPI (blue fluorescence). Scale bars: 20 μm.

4. Discussion

This study demonstrates that mucociliary transport activities of CRSwNP patients are suppressed in their nasal polyp mucosae relative to those in the inferior turbinate mucosae, and that the functional deterioration may be related to transcriptional changes in the set of PCP proteins in epithelial ciliated cells. The sinonasal mucosa is one of the initial sites of interaction between the body and extrinsic inhaled pathogens [1,2]. Chronic rhinosinusitis (CRS) is one of the most common chronic inflammatory diseases and deeply affects quality-of-life (QOL) status [6] as a result of both local and systemic impairment. CRS is a heterogenous syndrome resulting from a dysfunctional interaction between various environmental factors and the host immune system [11]. Extensive scientific evidence has been accumulated that justifies the stratification of CRS by the recognition of detailed endotypes, i.e., definition by the presence of particular patterns of immune cells and/or biomarkers [5,7–9], and the concept has in turn opened a new era of discovering and applying optimal treatment modalities for each phenotypic subset of CRS patients [10,11].

 doi:10.20944/preprints202407.1890.v1

Chronic rhinosinusitis with nasal polyps (CRSwNP) is a predominantly type 2-mediated inflammatory disease of the upper airway [5,13,20,39]. Type 2 inflammation is characterized by the presence of increased levels of the cytokines interleukin-(IL-)4, IL-5, and IL-13, and CCL26 as well as activation and recruitment of eosinophils and mast cells [11,14,15]. Patients with CRSwNP generally show a poor response to medical and surgical intervention compared to CRSsNP patients [17]. Persistent symptoms of severe CRSwNP include nasal blockage and nasal discharge, with patients frequently reporting altered sense of smell and taste [5,13,17–19]. The frequencies of various endotypes vary geographically around the world and even within a single country. For example, the type 2 profile has been the common endotype of CRSwNP in Western countries [40–42], whereas the majority of CRSwNP patients in Japan have shown neutrophil-dominant infiltration with the type 1 profile [14]. However, over the past decades, there has been an increase in the prevalence of Japanese patients showing type 2 CRSwNP phenotype accompanied by eosinophil-dominant inflammatory cell infiltration, much as in other allergic diseases such as asthma and allergic rhinitis [10,12,15,16]. Our data on patient demographics also show IL-13 and CCL26 as being elevated in the CRSwNP group with accompanying eosinophil infiltration, supporting the finding that type 2 inflammation is currently involved in the pathogenesis of NP formation [43].

Paranasal sinus cilia, which function under viscous and highly variable conditions, maintain their periodic motion even when subjected to certain degrees of external perturbation [3,26,44]. This function is dependent largely on the activity and coordination of the ciliary movement as well as on the number of cilia and the viscosity of periciliary mucus fluid. To maintain their mucus-transporting function under various conditions of viscosity, cilia must undergo periodic and asymmetric shape changes during their effective and recovery beating phases.

Structural remodeling of the nasal mucosa in CRSwNP consists of morphologic and functional changes to the epithelial cells, including proliferation of basal cells, hyperplasia of mucus-secreting goblet cells, and an epithelial–mesenchymal transition [5]. The changes trigger the loss of the differentiation ability of the ciliated cells [45] compromise the barrier function of the ciliated cells, thereby reducing the mucociliary clearance function. In the submucosal area of nasal polyps, degradation of the extracellular matrix and accompanying fibrin deposition and tissue edema lead to loss of structural integrity. Abnormal and excessive deposition of fibrin and retention of plasma proteins also occur and contribute to the increased viscosity and adherence of secreted mucus [46].

Based on pathological mechanisms occurring in the NP submucosa, it is an interesting question how the synchronicity of ciliary movement is affected through the changes in PCP expression. Our study suggests that the mucociliary transport function is impaired in nasal polyps. While ciliary movement in the inferior turbinate was directed posteriorly and downward, variations in direction were observed in nasal polyps. This indicates a disruption of the PCP pathway in nasal polyps. However, the mechanism underlying the poor ciliation and cilia dysfunction is still unclear.

Patients with CRSwNP are exposed to repeated cycles of inflammation and infection, which result in severe cilia loss and increased mucus secretion. In addition to direct ciliary loss, the surviving cilia that have experienced inflammatory and/or microbial damage may become dysfunctional [23,26,27]. The present study demonstrates that the mucociliary transport function is suppressed in nasal polyps compared to turbinate mucosae. The mean MCTV of nasal polyps was 98.6 μm/min, which was significantly less than that of the inferior turbinate mucosae (210.8 μm/min, $p < 0.01$). Further, the MCTV vector distribution differed between the two groups. Mucosal strips of the lateral side of the inferior turbinate showed steady transport ability in the posterior direction, whereas the vectors of nasal polyp specimens failed to maintain steady alignments and amplitudes. In human inferior turbinates, the epithelial layer of the lateral side generally retains its characteristic mucosal architecture without evidence of tissue destruction [47]. The MCC direction was pointed posteriorly in most turbinate mucosae in our patients, which was consistent with findings of a previous report [48] as well as other in vivo observational studies in humans using various tracers, such as saccharin, radioisotopes, and dyes [49–52].

Potential differences in ciliary beat frequency (CBF) function and MCC abilities in the nasal polyp tissues have been a matter of debate for decades. Several studies have reported that ciliated

 doi:10.20944/preprints202407.1890.v1

cells of nasal polyp explants showed vigorous ciliary movement *ex vivo*, identical to that of normal nasal mucosae [53–55]. Slater et al. analyzed CBF of the collected fragments of ciliated cell clusters by a photometric method from patients with nasal polyposis and normal volunteers. They found that the CBF of the patients was approximately equivalent to that of normal volunteers [56]. Bleier et al. [57] also reported no significant difference in the baseline CBF of cultured ciliated cells between CRSwNP patients and subjects without CRS. On the other hand, Li et al. [58] measured the CBF of cultured human nasal ciliated cells and found that cells isolated from nasal polyps exhibited lower baseline CBF than those from the inferior turbinates of subjects without CRS. The present finding of attenuated MCTV accompanying the loss of cilia synchronization in nasal polyps substantiates the above-mentioned proposal that MCC is suppressed even though active mucociliary beating is maintained in nasal polyps [59].

Ultrastructural studies of the inferior turbinate mucosae have previously highlighted the range of "normal" appearances of the lining of the nasal cavity at this site, with various proportions of ciliated cells covering the anterior end and lateral surface. Other cell types found include microvillous cells, secretory goblet cells, and squamous cells [35]. Previous studies of the ultrastructure of nasal polyps also documented various types of cilia abnormality that had been linked with inflammatory conditions [60]. In the present study, the inferior turbinate mucosae were mostly covered with well-preserved ciliated cells in both CRS and control subjects. Ciliary synchronization characterized by the typical metachronal pattern in SEM morphology was generally well-maintained in this area. On the other hand, the nasal polyp mucosae showed wide variation in the relative proportion of cell types among specimens. The degree of cilia synchronization varied and was relatively poor, with random orientation suggesting disorder in the arrangement of ciliated cells.

The PCP is acquired during differentiation of ciliated cells from basal cells and is essential to regulating the epithelial tissue integrity. In order to constitute this coordinated beating, the epithelial ciliated cells are arranged in an orderly fashion in which a specific signaling pathway of the PCP-related proteins is involved. A series of recent studies of proteomic and genetic analysis with imaging techniques have elucidated that a complex of structurally closely linked proteins called CPLANE (ciliogenesis and planar cell polarity effector) [61,62] are the main components responsible for planar cell polarity. These are the Inturned, Fuzzy and WDPCP proteins [29–32] and were once considered to promote the assembly of the cilium in the ciliogenesis process [63,64]. It remains a matter of debate whether these CPLANE proteins directly regulate the beating of cilia since aberrant short cilia are known to contribute to cilia beating dysfunction [33].

There are other pairs of proteins that control ciliogenesis and cilia function in the PCP pathway. Frizzled and Dishevelled are core PCP proteins that constitute one of the Wnt signaling pathways—i.e., the noncanonical Wnt/PCP pathway [65], which plays a role in the PCP formation. Frizzled and Dishevelled are eccentrically localized on a specific side of the apical surface of the cells [66–68]. Vangl and Prickle are another pair of core PCP proteins involved in the noncanonical Wnt/PCP pathway. Vangl is a four-span transmembrane protein, and Prickle is a cytoplasmic protein that binds to the intracellular domain of Vangl [65,69].

A prior study by Vladar et al. reported that organized production of these PCP proteins together with proper ciliary orientation is tightly linked to the process of normal ciliary differentiation/formation in human airway mucosae [59]. They propose that in chronic inflammatory diseases such as CRSwNP, suppression of the noncanonical Wnt/PCP pathway in ciliated epithelia leads to derangement of the direction of ciliary beating in neighboring ciliated cells. Ma et al. also observed that low expression of WDPCP in nasal polyps was accompanied with a decreased-frequency cilia beat pattern [70]. And in ALI cultures of human sinonasal epithelial cells (HSECs), there was a decrease in CBF following WDPCP silencing. These data suggest that in addition to its role in ciliogenesis, WDPCP is also critical to the cilia beating function. So far, few studies have linked FUZ to CRS pathology. This is a subject for future research because FUZ constitutes another part of the CPLANE complex along with WDPCP.

Nguyen et al. recently reported an intriguing finding of decreased MCC despite vigorous ciliary beating in NP mucosae of CRS patients accompanied by decreased PCP expressions [71]. They

 doi:10.20944/preprints202407.1890.v1

observed that the immunohistochemical expressions of Dishevelled, Frizzled, Prickle and Vangl isoforms were lower in nasal polyps than in the turbinate mucosae. Decreases of Dishevelled-1, Dishevelled-3 and Frizzled-3 in the nasal polyps were also observed at the transcriptional level. Consequently, the NP mucosae failed to exert an efficient mucociliary transport function, despite the competency of active ciliary beating. These data are consistent with ours, suggesting that the PCP pathway is more or less impaired in the ciliated cells of nasal polyps.

In the present study, the mRNA levels of WDPCP and FUZ were significantly lower in NP mucosae than in the ethmoid sinus mucosae. We further examined whether there was correlation between the expression of PCP-related proteins and other inflammatory cytokines. We confirmed that type 2 inflammatory cytokines were elevated in CRSwNP patients and found a close positive correlation between WDPCP and FUZ in the environment. To date there are no studies on the possible effects of type 2 inflammation on CPLANE expression. The relationship of CPLANE expressions with additional factors contributing to type 2 inflammations, such as eosinophil infiltration and FeNO levels, should be investigated.

We also examined the tissue distributions of WDPCP proteins by immunohistochemistry. Predominant positive WDPCP expression was located mostly in the ciliated cells. LSCM images showed that WDPCP protein was observed in the cytoplasmic region of ciliated cells and colocalized with ac-tubulin protein. These findings are consistent with previous reports and support the theory that WDPCP is involved in the PCP pathway of the sinonasal ciliary function [70].

The chronic inflammatory processes associated with CRSwNP result in cellular changes and structural remodeling of the nasal mucosa. These changes consist of morphologic and functional changes to the nasal epithelial cells, including proliferation of basal cells, hyperplasia of mucus-secreting goblet cells, and an epithelial–mesenchymal transition with loss of differentiation into ciliated cells at the mucosal surface [45]. These alterations, together with the present findings of decreased WDPCP distribution in the ciliated cells, compromise the barrier function and the regenerative capacity of the sinonasal epithelium and reduce mucociliary clearance. Further studies including a quantitative analysis of WDPCP expression levels are warranted to elucidate differences in MCC function between different CRS phenotypes.

This study has several limitations. First, the study included a relatively small number of Japanese patients; hence, caution should be taken when extrapolating our results to other ethnic groups. Further prospective studies on a larger scale are requisite to elucidate the function of the CPLANE complex. Second, because our results of MCTV were based on in vitro settings without CBF measurements, they may have not have adequately modeled the real-world environment of the sinonasal mucosa in CRS patients and control subjects. Finally, although there is heterogeneity in the endotypes of CRSwNP, such as type 1 or type 3, we did not analyze the subendotypes separately in this study.

5. Conclusions

Disruption of the PCP pathway in nasal polyps may hamper the maintenance of directionality necessary for typical ciliary synchronization, leading to a breakdown of MCC. This may be the cause of the decreased clearance and potential for worsening symptoms of CRS with nasal polyps. Pursuing therapeutic approaches to MCC dysfunction through the restoration of MCC may lead to new treatment options for CRSwNP patients (**Figure 9**).

 doi:10.20944/preprints202407.1890.v1

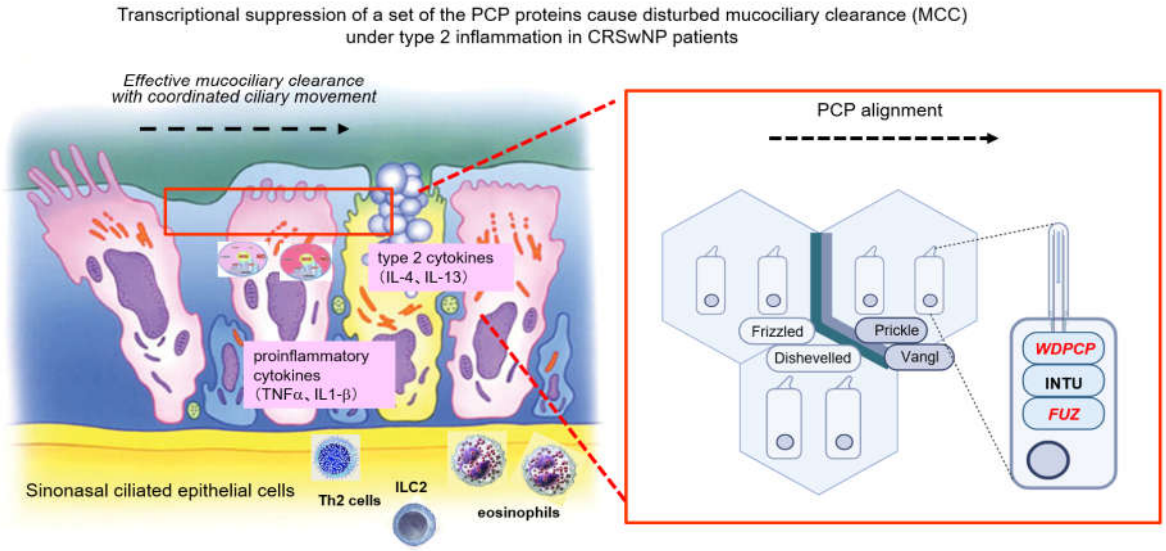

Figure 9. Graphical summary of the study. MCC constitutes the airway's primary innate physical defense against inhaled pathogens and irritants. Constant beating of motile cilia drives the pathogen-laden mucus toward the pharynx. Disruption of the PCP pathway in nasal polyps disrupts ciliary synchronization and leads to a breakdown of MCC.

Author Contributions: Conceptualization, S.H. and S.T.; methodology, T.K.; validation, T.H. and T.U.; formal analysis, S.H. and S.T.; investigation, S.H., T.K., Y.O., S.M., R.H., C.I., T.O. and Y.H.; resources, S.T. and T.K.; data curation, T.I.; writing—original draft preparation, S.H.; writing—review and editing, S.T.; visualization, S.H. and S.M.; supervision, S.T.; project administration, S.T.; funding acquisition, T.K. and S.T.

Funding: This research was supported by a grant from the Japan Society for the Promotion of Science KAKENHI (no. 22K09668 and no. 23K19659), and a Health Labor Sciences Research grant (H30-Nanchitou (Nan)-Ippan-016).

Institutional Review Board Statement: This study was performed in accord with the Declaration of Helsinki, with approval from the Institutional Review Board at the Hiroshima University School of Medicine (approval no. Hi-136-4; approval date: 2 Nov. 2022).

Informed Consent Statement: Written informed consent was obtained from all participants involved in the study.

Data Availability Statement: The data presented in this study are available on reasonable request from the corresponding author.

Acknowledgments: We thank Kaoru Shingai for technical assistance.

Conflicts of Interest: The authors declare no conflict of interest.

References

1. Cohen, N.A. Sinonasal mucociliary clearance in health and disease. *Ann. Otol. Rhinol. Laryngol. Suppl.* **2006**, 196, 20-6. doi: 10.1177/00034894061150s904. PMID: 17040014.
2. Hamilos, D.L. Host-microbial interactions in patients with chronic rhinosinusitis. *J. Allergy Clin. Immunol.* **2013**, 131, 1263-4, 1264.e1-6. doi: 10.1016/j.jaci.2013.02.020. PMID: 23540620.
3. Teff, Z.; Priel, Z.; Gheber, L.A. The forces applied by cilia depend linearly on their frequency due to constant geometry of the effective stroke. *Biophys. J.* **2008**, 94, 298-305. doi: 10.1529/biophysj.107.111724. PMID: 17872955.
4. Majima, Y.; Kurono, Y.; Hirakawa, K.; Suzaki, H.; Haruna, S.; Kawauchi, H.; Ichimura, K.; Moriyama, H. Reliability and validity assessments of a Japanese version of QOL 20-Item Sino-Nasal Outcome Test for chronic rhinosinusitis. *Auris Nasus Larynx.* **2010**, 37, 443-8. doi: 10.1016/j.anl.2009.11.016. PMID: 20197225.
5. Kato, A.; Schleimer, R.P.; Bleier, B.S. Mechanisms and pathogenesis of chronic rhinosinusitis. *J. Allergy Clin. Immunol.* **2022**, 149, 1491-1503. doi: 10.1016/j.jaci.2022.02.016. PMID: 35245537.

6. Metson, R.B.; Gliklich, R.E. Clinical outcomes in patients with chronic sinusitis. *Laryngoscope* **2000**, 110, 24-8. doi: 10.1097/00005537-200003002-00007. PMID: 10718411.
7. Dennis, S.K.; Lam, K.; Luong, A. A Review of Classification Schemes for Chronic Rhinosinusitis with Nasal Polyposis Endotypes. *Laryngoscope Investig. Otolaryngol.* **2016**, 1, 130-134. doi: 10.1002/lio2.32. PMID: 27917403.
8. Cho, S.H.; Bachert, C.; Lockey, R.F. Chronic Rhinosinusitis Phenotypes: An Approach to Better Medical Care for Chronic Rhinosinusitis. *J. Allergy Clin. Immunol. Pract.* **2016**, 4, 639-42. doi: 10.1016/j.jaip.2016.05.007. PMID: 27393778.
9. Grayson, J.W.; Hopkins, C.; Mori, E.; Senior, B.; Harvey, R.J. Contemporary Classification of Chronic Rhinosinusitis Beyond Polyps vs No Polyps: A Review. *JAMA Otolaryngol. Head Neck Surg.* **2020**, 146, 831-838. doi: 10.1001/jamaoto.2020.1453. PMID: 32644117.
10. Tokunaga, T.; Sakashita, M.; Haruna, T.; Asaka, D.; Takeno, S.; Ikeda, H.; Nakayama, T.; Seki, N.; Ito, S.; Murata, J.; et al. Novel scoring system and algorithm for classifying chronic rhinosinusitis: the JESREC Study. *Allergy* **2015**, 70, 995-1003. doi: 10.1111/all.12644. PMID: 25945591.
11. Fokkens, W.J.; Lund, V.J.; Hopkins, C.; Hellings, P.W.; Kern, R.; Reitsma, S.; Toppila-Salmi, S.; Bernal-Sprekelsen, M.; Mullol, J.; Alobid, I.; et al. European Position Paper on Rhinosinusitis and Nasal Polyps 2020. *Rhinology* **2020**, 58, 1-464. doi: 10.4193/Rhin20.600. PMID: 32077450.
12. Takeno, S.; Hirakawa, K.; Ishino, T. Pathological mechanisms and clinical features of eosinophilic chronic rhinosinusitis in the Japanese population. *Allergol. Int.* **2010**, 59, 247-256. doi: 10.2332/allergolint.10-RAI-0202. PMID: 20567131.
13. Fujieda, S.; Imoto, Y.; Kato, Y.; Ninomiya, T.; Tokunaga, T.; Tsutsumiuchi, T.; Yoshida, K.; Kidoguchi, M.; Takabayashi, T. Eosinophilic chronic rhinosinusitis. *Allergol. Int.* **2019**, 68, 403-412. doi: 10.1016/j.alit.2019.07.002. PMID: 31402319.
14. Khan, A.; Vandeplas, G.; Huynh, T.M.T.; Joish, V.N.; Mannent, L.; Tomassen, P.; Van Zele, T.; Cardell, L.O.; Arebro, J.; Olze, H.; et al. The Global Allergy and Asthma European Network (GALEN rhinosinusitis cohort: a large European cross-sectional study of chronic rhinosinusitis patients with and without nasal polyps. *Rhinology* **2019**, 57, 32-42. doi: 10.4193/Rhin17.255. PMID: 29911211.
15. Ishino, T.; Takeno, S.; Takemoto, K.; Yamato, K.; Oda, T.; Nishida, M.; Horibe, Y.; Chikuie, N.; Kono, T.; Taruya, T.; et al. Distinct Gene Set Enrichment Profiles in Eosinophilic and Non-Eosinophilic Chronic Rhinosinusitis with Nasal Polyps by Bulk RNA Barcoding and Sequencing. *Int. J. Mol. Sci.* **2022**, 23, 5653. doi: 10.3390/ijms23105653. PMID: 35628459.
16. Inoue, N.; Hirota, T.; Hatano, A.; Nakano, M.; Nakashima, D.; Nakayama, T.; Tamari, M.; Yoshikawa, M. Clinical characteristics in Japanese patients with chronic rhinosinusitis who underwent endoscopic sinus surgery. *Auris Nasus Larynx.* **2024**, 51, 286-294. doi: 10.1016/j.anl.2023.09.007. PMID: 37839999.
17. Soler, Z.M.; Sauer, D.; Mace, J.; Smith, T.L. Impact of mucosal eosinophilia and nasal polyposis on quality-of-life outcomes after sinus surgery. *Otolaryngol. Head Neck Surg.* **2010**, 142, 64-71. doi: 10.1016/j.otohns.2009.10.005. PMID: 20096225.
18. Abdalla, S.; Alreefy, H.; Hopkins, C. Prevalence of sinonasal outcome test (SNOT-22) symptoms in patients undergoing surgery for chronic rhinosinusitis in the England and Wales National prospective audit. *Clin. Otolaryngol.* **2012**, 37, 276-82. doi: 10.1111/j.1749-4486.2012.02527.x. PMID: 22776038.
19. Lin, Y.T.; Yeh, T.H. Studies on Clinical Features, Mechanisms, and Management of Olfactory Dysfunction Secondary to Chronic Rhinosinusitis. *Front. Allergy* **2022**, 3, 835151. doi: 10.3389/falgy.2022.835151. PMID: 35386650.
20. Stevens, W.W.; Schleimer, R.P.; Kern, R.C. Chronic Rhinosinusitis with Nasal Polyps. *J. Allergy Clin. Immunol. Pract.* **2016**, 4, 565-72. doi: 10.1016/j.jaip.2016.04.012. PMID: 27393770.
21. Kawasumi, T.; Takeno, S.; Ishikawa, C.; Takahara, D.; Taruya, T.; Takemoto, K.; Hamamoto, T.; Ishino, T.; Ueda, T. The Functional Diversity of Nitric Oxide Synthase Isoforms in Human Nose and Paranasal Sinuses: Contrasting Pathophysiological Aspects in Nasal Allergy and Chronic Rhinosinusitis. *Int. J. Mol. Sci.* **2021**, 22, 7561. doi: 10.3390/ijms22147561. PMID: 34299181.
22. Kuek, L.E.; McMahon, D.B.; Ma, R.Z.; Miller, Z.A.; Jolivert, J.F.; Adappa, N.D.; Palmer, J.N.; Lee, R.J. Cilia Stimulatory and Antibacterial Activities of T2R Bitter Taste Receptor Agonist Diphenhydramine: Insights into Repurposing Bitter Drugs for Nasal Infections. *Pharmaceuticals (Basel)* **2022**, 15, 452. doi: 10.3390/ph15040452. PMID: 35455449.
23. Wang, W.; Xu, Y.; Wang, L.; Zhu, Z.; Aodeng, S.; Chen, H.; Cai, M.; Huang, Z.; Han, J.; Wang, L.; et al. Single-cell profiling identifies mechanisms of inflammatory heterogeneity in chronic rhinosinusitis. *Nat. Immunol.* **2022**, 23, 1484-1494. doi: 10.1038/s41590-022-01312-0. PMID: 36138182.
24. Ha, J.G.; Cho, H.J. Unraveling the Role of Epithelial Cells in the Development of Chronic Rhinosinusitis. *Int. J. Mol. Sci.* **2023**, 24, 14229. doi: 10.3390/ijms241814229. PMID: 37762530.
25. Huang, Z.Q.; Liu, J.; Sun, L.Y.; Ong, H.H.; Ye, J.; Xu, Y.; Wang, D.Y. Updated epithelial barrier dysfunction in chronic rhinosinusitis: Targeting pathophysiology and treatment response of tight junctions. *Allergy* **2024**, 79, 1146-1165. doi: 10.1111/all.16064. PMID: 38372149.

26. Wanner, A.; Salathé, M.; O'Riordan, T.G. Mucociliary clearance in the airways. *Am. J. Respir. Crit. Care Med.* **1996**, 154, 1868-902. doi: 10.1164/ajrccm.154.6.8970383. PMID: 8970383..
27. Zhao, K.Q.; Cowan, A.T.; Lee, R.J.; Goldstein, N.; Droguett, K.; Chen, B.; Zheng, C.; Villalon, M.; Palmer, J.N.; Kreindler, J.L.; et al. Molecular modulation of airway epithelial ciliary response to sneezing. *FASEB J.* **2012**, 26, 3178-87. doi: 10.1096/fj.11-202184. PMID: 22516297.
28. Kim, S.K.; Shindo, A.; Park, T.J.; Oh, E.C.; Ghosh, S.; Gray, R.S.; Lewis, R.A.; Johnson, C.A.; Attie-Bittach ,T.; Katsanis, N.; et al. Planar cell polarity acts through septins to control collective cell movement and ciliogenesis. *Science* **2010**, 329, 1337-40. doi: 10.1126/science.1191184. PMID: 20671153.
29. Gray, R.S.; Abitua, P.B.; Wlodarczyk, B.J.; Szabo-Rogers, H.L.; Blanchard, O.; Lee, I.; Weiss, G.S.; Liu, K.J.; Marcotte, E.M.; Wallingford, J.B.; et al. The planar cell polarity effector Fuz is essential for targeted membrane trafficking, ciliogenesis and mouse embryonic development. *Nat. Cell Biol.* **2009**, 11, 1225-32. doi: 10.1038/ncb1966. PMID: 19767740.
30. Cui, C.; Chatterjee, B.; Lozito, T.P.; Zhang, Z.; Francis, R.J.; Yagi, H.; Swanhart, L.M.; Sanker, S.; Francis, D.; Yu, Q.; et al. Wdpcp, a PCP protein required for ciliogenesis, regulates directional cell migration and cell polarity by direct modulation of the actin cytoskeleton. *PLoS. Biol.* **2013**, 11, e1001720. doi: 10.1371/journal.pbio.1001720. PMID: 24302887.
31. Park, T.J.; Kim, S.K.; Wallingford, J.B. The planar cell polarity effector protein Wdpcp (Fritz) controls epithelial cell cortex dynamics via septins and actomyosin. *Biochem. Biophys. Res. Commun.* **2015**, 456, 562-6. doi: 10.1016/j.bbrc.2014.11.078. PMID: 25436430.
32. Ma, Y.; Sun, Y.; Jiang, L.; Zuo, K.; Chen, H.; Guo, J.; Chen, F.; Lai, Y.; Shi, J. WDPCP regulates the ciliogenesis of human sinonasal epithelial cells in chronic rhinosinusitis. *Cytoskeleton (Hoboken)* **2017**, 74, 82-90. doi: 10.1002/cm.21351. PMID: 28001338.
33. Bottier, M.; Thomas, K.A.; Dutcher, S.K.; Bayly, P.V. How Does Cilium Length Affect Beating? *Biophys. J.* **2019**, 116, 1292-1304. doi: 10.1016/j.bpj.2019.02.012. PMID: 30878201.
34. Takemoto, K.; Lomude, LS.; Takeno, S.; Kawasumi, T.; Okamoto, Y.; Hamamoto, T.; Ishino, T.; Ando, Y.; Ishikawa, C.; Ueda, T. Functional Alteration and Differential Expression of the Bitter Taste Receptor T2R38 in Human Paranasal Sinus in Patients with Chronic Rhinosinusitis. *Int. J. Mol. Sci*. **2023**, 24, 4499. doi: 10.3390/ijms24054499. PMID: 36901926.
35. Lund, V.J.; Kennedy, D.W. Quantification for staging sinusitis. The Staging and Therapy Group. *Ann. Otol. Rhinol. Laryngol. Suppl.* **1995**, 167, 17-21. PMID: 7574265.
36. Wake, M.; Takeno, S.; Hawke, M. The uncinate process: a histological and morphological study. *Laryngoscope* **1994**, 104, 364-9. doi: 10.1288/00005537-199403000-00020. PMID: 8127195.
37. Sonoyama, T.; Ishino, T.; Takemoto, K.; Yamato, K.; Oda, T.; Nishida, M.; Horibe, Y.; Chikuie, N.; Kono, T.; Taruya, T.; et al. Deep Association between Transglutaminase 1 and Tissue Eosinophil Infiltration Leading to Nasal Polyp Formation and/or Maintenance with Fibrin Polymerization in Chronic Rhinosinusitis with Nasal Polyps. *Int. J. Mol. Sci.* **2022**, 23, 12955. doi: 10.3390/ijms232112955. PMID: 36361742.
38. Ishikawa, C.; Takeno, S.; Okamoto, Y.; Kawasumi, T.; Kakimoto, T.; Takemoto, K.; Nishida, M.; Ishino, T.; Hamamoto, T.; Ueda, T.; et al. Oncostatin M's Involvement in the Pathogenesis of Chronic Rhinosinusitis: Focus on Type 1 and 2 Inflammation. *Biomedicines* **2023**, 11, 3224. doi: 10.3390/biomedicines11123224. PMID: 38137445.
39. Schleimer, R.P. Immunopathogenesis of Chronic Rhinosinusitis and Nasal Polyposis. *Annu. Rev. Pathol.* ***2017***, 12, 331-357. doi: 10.1146/annurev-pathol-052016-100401. PMID: 27959637.
40. Wang, X.; Zhang, N.; Bo, M.; Holtappels, G.; Zheng, M.; Lou, H.; Wang, H.; Zhang, L.; Bachert, C. Diversity of TH cytokine profiles in patients with chronic rhinosinusitis: A multicenter study in Europe, Asia, and Oceania. *J. Allergy Clin. Immunol.* **2016**, 138, 1344-1353. doi: 10.1016/j.jaci.2016.05.041. PMID: 27544740.
41. Lou, H.; Zhang, N.; Bachert, C.; Zhang, L. Highlights of eosinophilic chronic rhinosinusitis with nasal polyps in definition, prognosis, and advancement. *Int. Forum Allergy Rhinol.* **2018**, 8, 1218-1225. doi: 10.1002/alr.22214. PMID: 30296011.
42. Stevens, W.W.; Peters, A.T.; Tan, B.K.; Klingler, A.I.; Poposki, J.A.; Hulse, K.E.; Grammer, L.C.; Welch, K.C.; Smith, S.S.; Conley, D.B.; et al. Associations Between Inflammatory Endotypes and Clinical Presentations in Chronic Rhinosinusitis. *J. Allergy Clin. Immunol. Pract.* **2019**, 7, 2812-2820.e3. doi: 10.1016/j.jaip.2019.05.009. PMID: 31128376.
43. Bachert, C.; Hicks, A.; Gane, S.; Peters, A.T.; Gevaert, P.; Nash, S.; Horowitz, J.E.; Sacks, H.; Jacob-Nara, J.A. The interleukin-4/interleukin-13 pathway in type 2 inflammation in chronic rhinosinusitis with nasal polyps. *Front. Immunol.* **2024**, 15, 1356298. doi: 10.3389/fimmu.2024.1356298. PMID: 38690264.
44. Ikegami, K.; Sato, S.; Nakamura, K.; Ostrowski, L.E.; Setou, M. Tubulin polyglutamylation is essential for airway ciliary function through the regulation of beating asymmetry. *Proc. Natl. Acad. Sci. USA* **2010**, 107, 10490-5. doi: 10.1073/pnas.1002128107. PMID: 20498047.
45. Lee, K.; Tai, J.; Lee, S.H.; Kim, T.H. Advances in the Knowledge of the Underlying Airway Remodeling Mechanisms in Chronic Rhinosinusitis Based on the Endotypes: A Review. *Int. J. Mol. Sci.* **2021**, 22, 910. doi: 10.3390/ijms22020910. PMID: 33477617.

46. Takabayashi, T.; Schleimer, R.P. Formation of nasal polyps: The roles of innate type 2 inflammation and deposition of fibrin. *J. Allergy Clin. Immunol.* **2020**, 145, 740-750. doi: 10.1016/j.jaci.2020.01.027. PMID: 32145873.
47. Berger, G.; Gass, S.; Ophir, D. The histopathology of the hypertrophic inferior turbinate. *Arch. Otolaryngol. Head Neck Surg.* **2006**, 132, 588-94. doi: 10.1001/archotol.132.6.588. PMID: 16785402.
48. Do HB, Ohbuchi T, Yokoyama M, Kitamura T, Wakasugi T, Ohkubo JI, Suzuki H. Decreased ciliary beat responsiveness to acetylcholine in the nasal polyp epithelium. Clin Otolaryngol. 2019 May;44(3):356-365. doi: 10.1111/coa.13312. Epub 2019 Mar 18. PMID: 30762948.
49. Kaya, S.; Ercan, M.T.; Laleli, Y. Measurement of nasal mucociliary activity in man with 99mTc-labelled resin particles. *Arch. Otorhinolaryngol.* **1984**, 239, 267-72. doi: 10.1007/BF00464254. PMID: 6732603.
50. Passali, D.; Cappello, C.; Passali, G.C.; Cingi, C.; Sarafoleanu, C.; Bellussi, L.M. Nasal Muco-ciliary transport time alteration: efficacy of 18 B Glycyrrhetinic acid. *Multidiscip. Respir. Med.* **2017**, 12, 29. doi: 10.1186/s40248-017-0110-7. PMID: 29209499.
51. Paul, B.; Menon, S.S.; Vasthare, R.; Balakrishnan, R.; Acharya, S. Effect of bidi smoking on nasal mucociliary clearance: a comparative study. *J. Laryngol. Otol.* **2018**, 132, 1077-1082. doi: 10.1017/S0022215118002049. PMID: 30457082.
52. Sahin, E.; Hamamcı, M.; Kantekin, Y. Measurement of mucociliary clearance in the patients with multiple sclerosis. *Eur. Arch. Otorhinolaryngol.* **2020**, 277, 469-473. doi: 10.1007/s00405-019-05717-w. PMID: 31707467.
53. Zahm, J.M.; Pierrot, D.; Hinnrasky, J.; Fuchey, C.; Chevillard, M.; Gaillard, D.; Puchelle, E. Functional activity of ciliated outgrowths from cultured human nasal and tracheal epithelia. *Biorheology* **1990**, 27, 559-65. doi: 10.3233/bir-1990-273-434. PMID: 2261521.
54. Chevillard, M.; Hinnrasky, J.; Pierrot, D.; Zahm, J.M.; Klossek, J.M.; Puchelle, E. Differentiation of human surface upper airway epithelial cells in primary culture on a floating collagen gel. *Epithelial Cell Biol.* **1993**, 2, 17-25. PMID: 7689028.
55. Adam, E.C.; Schumacher, D.U.; Schumacher, U. Cilia from a cystic fibrosis patient react to the ciliotoxic Pseudomonas aeruginosa II lectin in a similar manner to normal control cilia--a case report. *J. Laryngol. Otol.* **1997**, 111, 760-2. doi: 10.1017/s0022215100138551. PMID: 9327018.
56. Slater, A.; Smallman, L.A.; Logan, A.C.; Drake-Lee, A.B. Mucociliary function in patients with nasal polyps. *Clin. Otolaryngol. Allied Sci.* **1996**, 21, 343-7. doi: 10.1111/j.1365-2273.1996.tb01084.x. PMID: 8889303.
57. Bleier, B.S.; Mulligan, R.M.; Schlosser, R.J. Primary human sinonasal epithelial cell culture model for topical drug delivery in patients with chronic rhinosinusitis with nasal polyposis. *J. Pharm. Pharmacol.* **2012**, 64, 449-56. doi: 10.1111/j.2042-7158.2011.01409.x. PMID: 22309277.
58. Li, Y.Y.; Li, C.W.; Chao, S.S.; Yu, F.G.; Yu, X.M.; Liu, J.; Yan, Y.; Shen, L.; Gordon, W.; Shi, L.; et al. Impairment of cilia architecture and ciliogenesis in hyperplastic nasal epithelium from nasal polyps. *J. Allergy Clin. Immunol.* **2014**, 134, 1282-1292. doi: 10.1016/j.jaci.2014.07.038. PMID: 25201258.
59. Vladar, E.K.; Nayak, J.V.; Milla, C.E.; Axelrod, J.D. Airway epithelial homeostasis and planar cell polarity signaling depend on multiciliated cell differentiation. *JCI Insight* **2016**, 1, e88027. doi: 10.1172/jci.insight.88027. PMID: 27570836.
60. Busuttil, A.; More, I.A.; McSeveney, D. A reappraisal of the ultrastructure of the human respiratory nasal mucosa. *J. Anat.* **1977**, 124, 445-58. PMID: 591439.
61. Pazour, G.J.; Agrin, N.; Leszyk, J.; Witman, G.B. Proteomic analysis of a eukaryotic cilium. *J. Cell Biol.* **2005**, 170, 103-13. doi: 10.1083/jcb.200504008. PMID: 15998802.
62. Toriyama, M.; Lee, C.; Taylor, S.P.; Duran, I.; Cohn, D.H.; Bruel, A.L.; Tabler, J.M.; Drew, K.; Kelly, M.R.; Kim, S.; et al. The ciliopathy-associated CPLANE proteins direct basal body recruitment of intraflagellar transport machinery. *Nat. Genet.* **2016**, 48, 648-56. doi: 10.1038/ng.3558. PMID: 27158779.
63. Park, T.J.; Haigo, S.L.; Wallingford, J.B. Ciliogenesis defects in embryos lacking inturned or fuzzy function are associated with failure of planar cell polarity and Hedgehog signaling. *Nat. Genet.* **2006**, 38, 303-11. doi: 10.1038/ng1753. PMID: 16493421.
64. Kim, S.K.; Shindo, A.; Park, T.J.; Oh, E.C.; Ghosh, S.; Gray, R.S.; Lewis, R.A.; Johnson, C.A.; Attie-Bittach, T.; Katsanis, N.; et al. Planar cell polarity acts through septins to control collective cell movement and ciliogenesis. *Science* **2010**, 329, 1337-40. doi: 10.1126/science.1191184. PMID: 20671153.
65. Vladar, E.K.; Königshoff, M. Noncanonical Wnt planar cell polarity signaling in lung development and disease. *Biochem. Soc. Trans.* **2020**, 48, 231-243. doi: 10.1042/BST20190597. PMID: 32096543.
66. Strutt, D.I. Asymmetric localization of frizzled and the establishment of cell polarity in the Drosophila wing. *Mol. Cell.* **2001**, 7, 367-75. doi: 10.1016/s1097-2765(01)00184-8. PMID: 11239465.
67. Axelrod, J.D. Unipolar membrane association of Dishevelled mediates Frizzled planar cell polarity signaling. *Genes. Dev.* **2001**, 15, 1182-7. doi: 10.1101/gad.890501. PMID: 11358862.
68. Vladar, E.K.; Bayly, R.D.; Sangoram, A.M.; Scott, M.P.; Axelrod, J.D. Microtubules enable the planar cell polarity of airway cilia. *Curr. Biol.* **2012**, 22, 2203-12. doi: 10.1016/j.cub.2012.09.046. PMID: 23122850.

69. Dreyer, C.A.; VanderVorst, K.; Carraway, K.L. 3rd. Vangl as a Master Scaffold for Wnt/Planar Cell Polarity Signaling in Development and Disease. *Front. Cell Dev. Biol.* **2022**, 10, 887100. doi: 10.3389/fcell.2022.887100. PMID: 35646914.
70. Ma, Y.; Tian, P.; Zhong, H.; Wu, F.; Zhang, Q.; Liu, X.; Dang, H.; Chen, Q.; Zou, H.; Zheng, Y. WDPCP Modulates Cilia Beating Through the MAPK/ERK Pathway in Chronic Rhinosinusitis With Nasal Polyps. *Front. Cell Dev. Biol.* **2021**, 8, 630340. doi: 10.3389/fcell.2020.630340. PMID: 33598458.
71. Nguyen, T.N.; Koga, Y.; Wakasugi, T.; Kitamura, T.; Suzuki, H. Nasal polyps show decreased mucociliary transport despite vigorous ciliary beating. *Braz. J. Otorhinolaryngol.* **2024**, 90, 101377. doi: 10.1016/j.bjorl.2023.101377. PMID: 38232516.